

Barbara K. Wilk

barbara.wilk@pg.edu.pl

Department of Water and Wastewater Technology, Gdansk University of Technology

Aleksander J. Urbański

Institute of Geotechnics, Cracow University of Technology

THE IMPACT OF THE SHAPE OF SCREEN OPENINGS ON GROUNDWATER
FLOW TO A DEEP DRILLED WELL

WPLYW KSZTAŁTU OTWORÓW FILTRU STUDNI GŁĘBINOWEJ NA PROCES
FILTRACJI W JEJ OTOCZENIU

Abstract

The authors propose a supplementary method for modelling seepage flow around a deep drilled well screen. The study applies 3D numerical modelling (FEM) in order to provide an in-depth analysis of the seepage process. The analysis of flow parameters (flux distribution $\mathbf{q}(\mathbf{x}, t)$ and pressure distribution p) was conducted using the ZSoil.PC software system. The analysis indicates that the shape of perforation is of secondary importance during deep bore well screen selection.

Keywords: deep drilled well screen, FEM, ZSoil, groundwater flow

Streszczenie

Autorzy proponują uzupełniającą metodę modelowania filtracji wokół filtru studni głębinowej. W pracy zastosowano modelowanie numeryczne 3D (MES) w celu dogłębnej analizy parametrów procesu filtracji. Analizę parametrów filtracji (rozkład prędkości filtracji $\mathbf{q}(\mathbf{x}, t)$ oraz rozkład ciśnienia p) przeprowadzono za pomocą systemu MES ZSoil.PC. Analiza wykazała, że kształt perforacji ma drugorzędne znaczenie podczas selekcji filtru studni głębinowej.

Słowa kluczowe: filtr studni wierconej, MES, ZSoil, filtracja

1. Introduction

Groundwater, accessed through deep drilled wells, usually supplies water of a quality superior to surface water [8, 23]. The groundwater is a valuable natural resource, readily used in, for example, industrial, medical or municipal applications [2, 26]. Moreover, groundwater resources are more accessible than surface water. Therefore, it is crucial to develop and broaden knowledge on the quantity and quality of groundwater, and on the appropriate methods for its withdrawal [13].

The correct usage of groundwater resources requires in-depth knowledge on the construction and operation of deep drilled wells [1]. It should be pointed out that a screen is one of the key elements of the drilled well as it helps to maintain the required well performance and deliver water free of a fine soil fraction [7]. Therefore, when designing a deep drilled well, its technical parameters must be carefully considered [20].

A thorough literature review on the design of deep drilled well screens failed to answer the question of whether the shape of a screen perforation has a significant impact on the performance of a screen. The review of the available literature has only led to the conclusion that the key technical parameters of a deep drilled well screen include the total screen surface (working surface) area, total area of screen openings and the size of the openings (depending on a size of the aquifer grain or a filter pack fill adhering to the screen).

It should also be stressed that thus far, analyses of seepage flow in the vicinity of deep drilled well screens have been based mainly on empirical formulas. The design groundwater inflow rates, determined by individually laboratories, have significantly differed from each other. Therefore, a detailed analysis of seepage related fields (flow distribution $\mathbf{q}(\mathbf{x}, t)$, pressure distribution $p(\mathbf{x}, t)$) was conducted using the ZSoil PC software, which employs the 3D numerical modelling methodology (FEM) and a homogenisation technique.

2. Groundwater flow in full saturation conditions

Seepage, as the movement of groundwater, is influenced by a variety of factors, such as: grading of soil, soil structure, soil porosity and cracking [2, 23]. The filtering properties are determined with the permeability coefficient k . Assuming a full saturation of the porous medium, the average flow q in a one-dimensional situation can be determined from the following formula, commonly known as Darcy's law [8]. Assuming that the fluid's viscosity, temperature and density are constant, this takes the form:

$$q = -k \cdot J \quad (1)$$

In this model, the seepage flow (Darcy velocity) is directly proportional to the hydraulic gradient J , and k is the proportionality coefficient. Darcy's law is applicable only to laminar flows and is invalid for rocks or soils with a very high permeability [8, 24, 14, 13]. These limitations of the validity of Darcy law can be expressed by the notion of dimensionless Reynolds number Re :



$$Re = \frac{\rho \cdot q \cdot d}{\eta} \quad (2)$$

where:

- ρ – water density,
- η – dynamic viscosity of ground water (= 0.0013 kg/m/s),
- d – diameter of flow channel.

In ground water seepage problems, parameter d corresponds to an average diameter of a ‘channel’ between solid soil particles. This characteristic dimension of a ground microstructure is related to soil porosity, grain sizes and its distribution curve. Different sources give different limiting values of Re preserving the laminar flow regime, with the range $Re = 1-10$ in Bear [3], to $Re = 30$ in Houben [10].

Considering a general, three-dimensional case with a constant permeability coefficient and an isotropic medium, the flow components can be calculated from the following formulas [18, 14]:

$$\mathbf{q} = -k \cdot \mathbf{grad}(p/\gamma_w + Y) \equiv q_i = -k(H+Y)_{,i} \quad (3)$$

where:

- γ_w – volumetric weight of the fluid,
- Y – the potential of the gravity field, which is negligible in the analysed flow homogenisation case (close to the screen).

However, it is important while analysing groundwater flow in macroscopic systems (e.g. while looking at a free surface close to the screen or at a flow distribution up the screen height). Darcy’s law, as a constitutive equation for seepage in a porous medium, must be supplemented by a balance equation, which in full saturation conditions, takes the following form:

$$\mathit{div} \mathbf{q} = \frac{\partial q_x}{\partial x} + \frac{\partial q_y}{\partial y} + \frac{\partial q_z}{\partial z} = 0 \equiv q_{i,i} = 0 \quad (4)$$

Expressing equation (4) through pressure p or hydraulic head H , Laplace’s equation is obtained:

$$\nabla^2 p = \frac{\partial^2 p}{\partial x^2} + \frac{\partial^2 p}{\partial y^2} + \frac{\partial^2 p}{\partial z^2} = 0 \equiv p_{,ii} = 0 \equiv H_{,ii} = 0 \quad (5)$$

This equation serves as the basis for a numerical analysis conducted using the finite elements method (FEM), which is discussed further in this paper. To solve the boundary problem, the conditions applicable to each point of the boundary of the calculation domain have to be determined. Thus, for the problem presented in Fig. 2, the first-type (Dirichlet) boundary condition (equation 6) applies to pressure (where its value is known, i.e. within the opening $\bar{p} = 0$ and $\bar{p} = 1$ on the outer surface:

$$p = \bar{p} \quad (6)$$

The second-type (Neumann) boundary condition, for the flow perpendicular to the boundary (equation 7), applies to the remaining parts of the periodic cell boundary, where



a lack of normal flow is caused by the presence of a filter pipe, or by flow symmetry and periodicity.

$$\mathbf{n} \cdot \mathbf{q} \equiv n_i q_i = q_n = \bar{q}_n = 0 \quad (7)$$

3. Screen in a deep drilled well

The screen is an element of the filter column which also comprises a subfilter pipe (which very often acts as a sedimentation basin) and an upper pipe, which connects the screen with the ground surface [20, 16]. The designing of deep drilled well screens focuses mainly on their following features: length, elevation, perforation, diameter and acceptable screen performance. The main objective of the screen is thus to let water pass from the aquifer into the well and prevent loose soil, sediment and rock from entering the well while minimising hydraulic resistance. With regard to the above, in the past, well screens were selected with the largest possible opening area (lowest entrance velocity) [14]. The most recent field experience and laboratory tests have shown that the average entrance velocity of water moving into the screen should not exceed 0.6-1.2 m/s (providing that the screens have open areas greater than 3-5%) [1, 5, 11, 16]. However, Water Well Construction Standard ANSI/NGWA-01-14 does not specify the maximum screen entrance velocity due to the fact that different variants of entrance velocity and screen open area can give similar values for the designed screen length [1, 11, 16]. Moreover, the document indicates that the perforation of the well screen should be as large as possible, providing a laminar flow entrance velocity.

The size of well screen perforation is also largely dependent on the type of aquifer and the use of a gravel pack [2, 19]. Additionally, well screens should be characterised by correct slot design to minimise blockage, they should be constructed from corrosion resistant material and have a structure that hinders the formation of sediments of mechanical, chemical or biochemical origin [18, 20]. They should also be designed to prevent sanding the well during its normal operation. A proper screen ensures longevity and trouble-free operation of the deep drilled well [13]. Therefore, the following types of screens may be used: framed screens, mesh screens, gravel screens, and various types of special structures (e.g. those constructed from porous concrete prefabricates).

The framed screens with a proper perforation are the most frequently used type of screen [14, 21].

4. Framed screen perforation

Framed well screens are usually in the form of pipes with a series of openings (of a specific shape) to enable water to pass through. The openings can be round or rectangular (slots) [14]. The diameters or widths of screen openings are selected according to the grain size of the aquifer. The Abramow's formulas can be applied to calculate the dimensions of the screen

openings based on the uniformity coefficient of grains of a filter layer, which is in a direct contact with the filter (η) [7, 15, 17, 20]. It should be noted that the diameter of openings should not be smaller than 10 mm and not larger than 25 mm. The slot width should not exceed 10 mm. When designing a framed screen perforation, the screen flow rate coefficient must be calculated from the following formula [13]:

$$m_f = \frac{f}{F} \quad (8)$$

where:

f – total area of the openings (active surface),

F – surface area with perforation, screen surface (working surface).

For round openings $m_f \leq 0.25$; for slots $m_f \leq 0.15$.

5. Materials & Methods

Modelling of a groundwater flow with the ZSoil.PC FEM software was preceded by calculations of technical parameters of a deep drilled well. The calculations were performed according to the groundwater intake design principles formulated by Wieczysty and Gabryszewski for the given input data. In this way, reliable and accurate data was obtained for further numerical calculations. Following the calculation of the screen length and diameter, the dimensions of three types of openings were determined. These were: round holes (chessboard), longitudinal slots and transversal slots. The openings were distributed on the screen surface and the total area of screen perforation was kept constant for each case. The appropriate filter pack grain size was selected to ensure that the grains did not pass through the screen, i.e. to protect the well against sand accumulation. Table 1 presents the conditions and results of further calculations in ZSoil.PC (FEM) (Table 1.).

Table 1. Input data and major results of deep drilled well screen calculations

Aquifer grain size	Screen openings	Water table	Calculated screen length, m	Calculated outer screen diameter, m	Calculated inner screen diameter, m	Calculated diameter of filter pack pipe ($d_{50} = 4.0$ mm), m
$d_{10} = 0.32$ mm $d_{30} = 0.35$ mm $d_{60} = 0.39$ mm	a) round hole perforation (chessboard) b) longitudinal slot perforation c) transversal slot perforation	Free water table 12 m BGL	2.80	0.195	0.175	0.395

Dimensions of the deep drilled well screen for the analysed options are provided below:



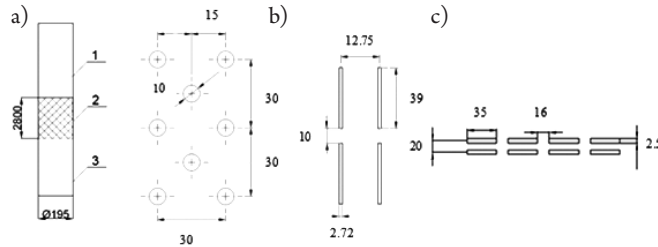


Fig. 1. Deep drilled well screen (1 – upper pipe, 2 – filter, 3 – subfilter pipe) with $mf = 8.35\%$: a) round hole perforation (chessboard), b) longitudinal slot perforation, c) transversal slot perforation; all dimensions in [mm]

After determining the screen size for the given application, the groundwater flow was determined for three deep drilled well screens, differing in screen opening shapes; flow rate coefficients for each option were kept constant ($mf \approx 8.35\%$). The numerical analysis was based on flow homogenisation, assuming its periodicity both along and around the pipe. The periodic cell was created and defined as a section of a hollow cylinder with an internal radius of $R1 = 97.5$ mm and filter pack dimensions of $a = 100$ mm; this was identical for each type of perforation. A radius of $R3 = 297.5$ mm, for the outer cell surface was selected for cases in which any visible fluctuations of the flux vector \mathbf{q} vanish.

Two permeability coefficients in the filter pack and the surrounding aquifer zone have been considered:

- 1) with different values: $k = 1.0$ [mm/s] = $1.0e^{-3}$ [m/s] for a filter pack, $k_1 = 0.01$ $k = 1.0e^{-5}$ [m/s] – for an aquifer strata, a medium sand was adopted in this study,
- 2) with a constant value of $k_1 = k = 1.0$ [mm/s] = $1.0e^{-3}$ [m/s] assumed in both zones.

It is worth noting that these are just approximate, indicative values, roughly corresponding to real numbers. Nevertheless, due to linearity of the boundary problem, the obtained results correctly illustrate the nature of the phenomenon, and could be generalised to other data; however, this can only be done if the conditions of Darcy law validity, described in p.1, hold.

The 3D FEM models of a periodic cell for the three types of openings with the adopted boundary conditions (p – pressure [kN/m²], q_n – flux normal to the surface) are shown in Fig. 2.

It is assumed that the depth of the screen tube wall is so small that pressure distribution along the segment between the inner and outer surface of a tube may be approximated by a sudden drop to a value of $p = 0$ on the outer surface of the screen tube, which is also the inner surface of the periodic cell.

6. Results and discussion

The pressure field was determined for all six analysed cases (3 x 2 conditions). The pressure distribution for the three perforation types is very similar, i.e. the closer to the centre of the opening, the lower the pressure; pressure increases with the distance from the perforation. In the case of flow

setups 1a, 1b and 1c, a significant disproportion (100 x) of the permeability coefficient between the highly permeable layer of the filter pack and the aquifer close to the pipe is observed. This disproportion causes a drop in the value of the pressure close to the pipe (Fig. 3).

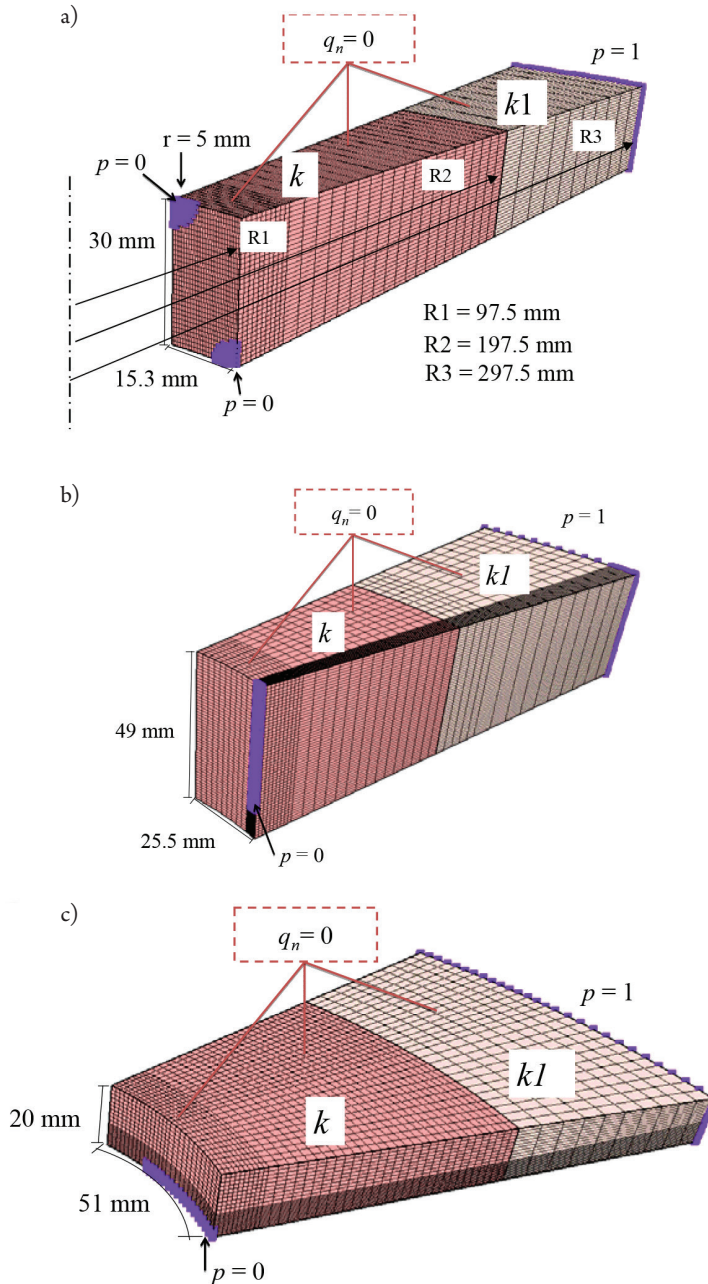


Fig. 2. A periodic cell of a deep drilled well screen with perforation and a screen adjacent zone: a) circular hole perforation, b) longitudinal slot perforation, c) transversal slot perforation

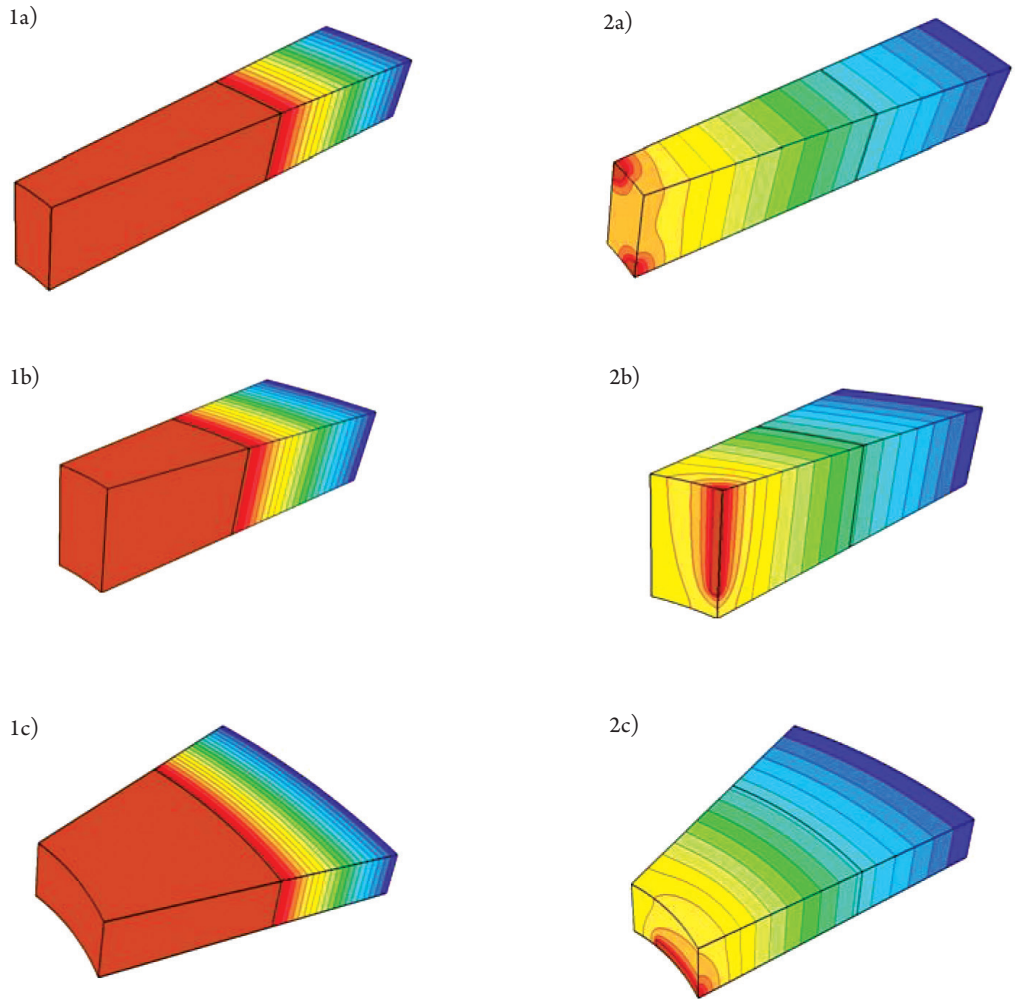


Fig. 3. Pressure distribution in the periodic cell: a) round hole perforation, b) longitudinal slot perforation, c) transversal slot perforation for both flow setups; maximum pressure value $p = 1 \text{ kN/mm}^2$ (dark blue), minimum pressure value $p = 0 \text{ kN/mm}^2$ (brown)

Numerical studies performed by a few authors [9, 13, 21, 22, 24] describe a drop in pressure in close proximity to the well screen. Szanyia et al. (2018) describe pressure distribution near the well screen (crude oil inflow to a horizontal drilling well), whereas the exact pressure distribution for different screen perforations has not been calculated on a micro-scale.

After specifying the boundary conditions, the results clearly indicate that the highest flow values were found at the well screen openings and in their immediate vicinity, also that they dropped with increasing distances from the screen openings. Additionally, the individual flux vectors $|\mathbf{q}|$ at the outer surface of the computational domain were read for each case presented below.

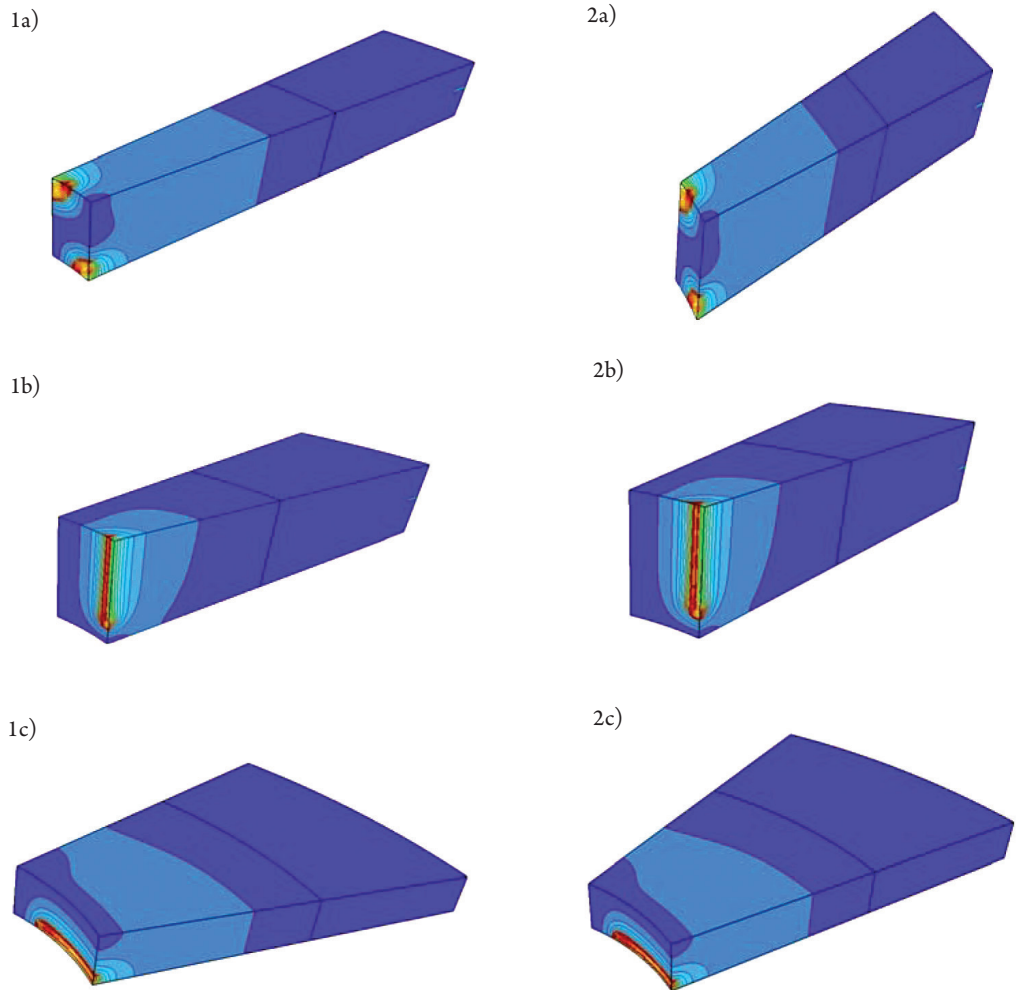


Fig. 4. Maps of individual flux vectors $|\mathbf{q}|$ distribution for three options of the periodic cell: a) round hole perforation, b) longitudinal slot perforation, c) transversal slot perforation

Table 2. Flow at the outer surface of the periodic cell (radius $R = 297$ mm)

perforation/set up of k type	1) $k_1 = 0.01$ $k = 0.01$ mm/s $ \mathbf{q} \times 10^{10}$ [mm/s]	2) $k = k_1 = 1$ mm/s $ \mathbf{q} \times 10^{10}$ [mm/s]
a) circular	0.08153	2.47384
b) vertical	0.08136	2.32901
c) transversal	0.08143	2.39139

Interestingly, the values of flux vectors $|\mathbf{q}|$ at the outer surface of the cell (Table 2), obtained for the same unit pressure value p , were very close to each other for all types of perforation.

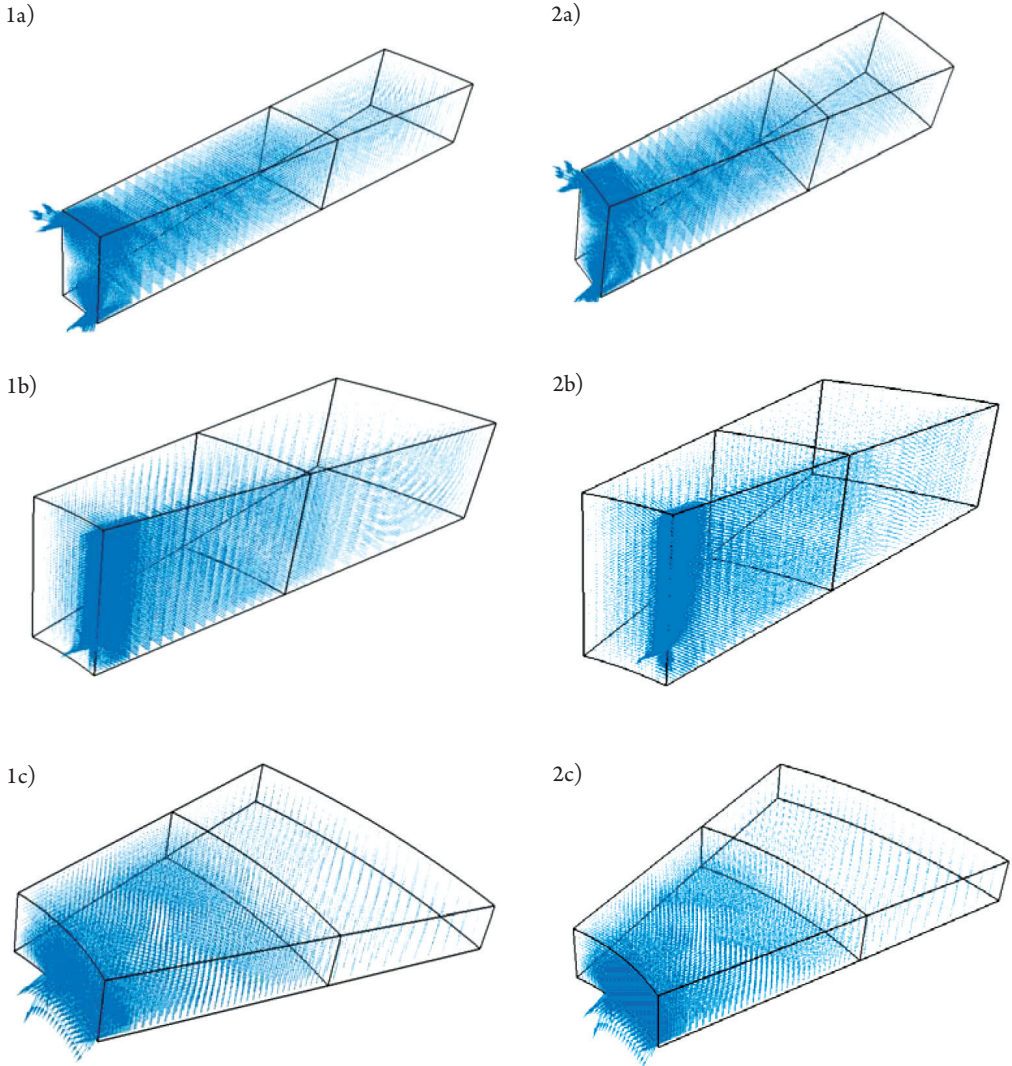


Fig. 5. Flux vectors $|\mathbf{q}|$ distribution for three options of the periodic cell: a) round hole perforation, b) longitudinal slot perforation, c) transversal slot perforation

Numerical modelling in the close proximity to the deep drilled well screen was discussed in several publications [13, 22, 24, 27]. However, the authors of the publications approach the subject differently due to the complexity of the issue and the diversity of situations that may occur in practice. Therefore, it is difficult to compare the results obtained in this publication with others. Most publications focus on determining the right water entrance velocity into the drilled well screen and there are many different opinions on this topic [6, 18, 10, 12, 15, 22]. There are also many publications on new analytical and numerical models explaining and quantifying the flow behaviour in aquifer systems [27]. These often include comparisons with analytical methods.

The currently available publications certainly confirm the results obtained by the authors with regard to the occurrence of the largest values of groundwater velocity vectors near the well screen. They also confirm the pressure distribution obtained in this publication and the distribution of flux vectors, although without taking into account the different types of perforation. The authors prove the abovementioned dependencies using other tools (e.g. Fluent program) and do not analyse it on a micro-scale.

It should be noted that the approach to the issue proposed by the authors is simplified, as it is based on Darcy's law (assumption of a laminar inflow into the well under full saturation conditions); however, it can be a good preliminary verification of empirical formulas, on the basis of which, the perforation of the screen is selected. It should be noted, however, that in close proximity to the screen, the groundwater flow may show some deviations from Darcy's law [11] and this will be covered in the next phase of authors research, along with other considerations. Other issue ignored are hydraulic losses at the openings, which in the case of the thin walls of the filter screen can be considered to be of minimal importance.

The presented computational analysis of seepage fields in a close neighbourhood of the screen (dimensions of finite elements are limited by slot width to 0.2 mm and analysis is performed on a domain of periodic cell with height $\sim 10^{-2}\text{m}$) can be seen as a micro-scale analysis, being the first step of a multi-scale analysis of the seepage problem. The obtained results can be easily used for the identification of permeability properties of special finite elements by homogenisation. These linear (1D) finite elements, described in ZSoil [29], can represent drilled wells in 3D FEM computational models of a macro-scale system reaching hundred of meters, see Urbański [24, 25].

7. Conclusions

The obtained results indicate that the m_f coefficient is the key parameter for the selection of the opening of a deep drilled well screen. If the m_f value is maintained, the shapes and the distribution of openings are of a secondary importance. The velocity and the pressure distributions are nearly identical for the studied cases. The highest flow values are observed at the centre of the screen openings and in its immediate vicinity; flow rate drops proportionally to the distance from the perforation.

The simulations with the three-dimensional FEM showed that the engineering formulas where flows to the screen depended only on the m_f coefficient were of the most practical use.

References

- [1] American Water Works Association, *AWWA Standard for Water Wells*. ANSI/NGWA-01-14, AWWA, Denver 2014.
- [2] Antoniou A., Smits F., Stuyfzand P., *Quality assessment of deep-well recharge applications in the Netherlands*, Water Science and Technology: Water Supply 17(5) /2017, 1201–1211.
- [3] Bear J., *Hydraulics of Groundwater*, Mineola, Dover 2007.

- [4] Boyraz U., Kazezyilmaz-Alhan C.M., *Solutions for groundwater flow with sloping stream boundary: analytical, numerical and experimental models*, Hydrology Research 4(48)/2017, 258–267.
- [5] Byung-Woo K., *Effect of Filter Designs on Hydraulic Properties and Well Efficiency*, Groundwater S1(52) /2014, 175–185.
- [6] Castellazzi P., Martel R., Galloway D.L., Longuevergne L., Rivera A., *Assessing Groundwater Depletion and Dynamics Using GRACE and InSAR: Potential and Limitations*, Groundwater, 54(6)/2016, 768–780.
- [7] Delleur J.W., *Elementary Groundwater Flow and Transport Processes, The Handbook of Groundwater Engineering*, Cushman, J. H. & Tartakovsky, D.M. (Eds.), CRC Press LLC, Florida 2016.
- [8] Gabryszewski T., Wieczysty A., *Ujęcia wód podziemnych*, Arkady, Warszawa 1985.
- [9] George R.M., *Bore Wells Vs. Open Wells: Water Crisis and Sustainable Alternatives in Kerala*, Journal of Management & Public Policy 7(2)/2016, 19–28.
- [10] Houben G.J., Hauschild S. I., *Numerical modelling of the near-field hydraulics of water wells*, Hydrogeology Journal 49(4)/2011, 570–575.
- [11] Houben G.J., *Hydraulics of water wells – flow laws and influence of geometry*, Hydrogeology Journal 23(8)/2015, 1633–1657.
- [12] Houben G.J., *Review: Hydraulics of water wells – head losses of individual components*, Hydrogeology Journal 23(8)/2015, 1659–1675.
- [13] Karatzas G.P., *Developments on Modeling of Groundwater Flow and Contaminant Transport*, Water Resources Management 31(10)/2017, 3235–3245.
- [14] Knapik K., Bajer J., *Wodociągi*, Politechnika Krakowska, Kraków 2011.
- [15] Lubowiecka T., *Mathematical model of deep drilled wells with confined aquifer and its empirical verification*, PhD dissertation, Cracow University of Technology, Kraków 1978.
- [16] Mahasneh A.M., *Well Screens and Gravel Packs*, Global Journal Of Science Frontier Research 15-5-H/2015, 30–39.
- [17] Manera D.B., Voltolini T.V., Menezes D.R., Leal de Araujo G.G., *Chemical Composition of Drilled Wells Water for Ruminants*, Journal of Agricultural Science 8(12)/2016, 127–132.
- [18] Mansuy N., *Water Well Rehabilitation: A Practical Guide to Understanding Well Problems and Solutions*, Layne Geosciences Inc., USA 1999.
- [19] Misstear B.D.R., Banks D., Clark L., *Water wells and boreholes*, Wiley, Chichester 2016.
- [20] Nanteza J., de Linage C.R., Thomas B.F., Famiglietti J.S., *Monitoring groundwater storage changes in complex basement aquifers: An evaluation of the GRACE satellites over East Africa*, Water Resources Research 52(12)/2016, 9542–9564.
- [21] Satora S., *Konstrukcje Studni Wierconych Ujmujących Wody Podziemne z Warstw Fliszowych*, III Konferencja Naukowo-Techniczna “Błękitny San”, Dubiecko, 21–22 kwietnia 2006.
- [22] Szanyi M.L., Hemmingsen, C.S., Yan, W., Walther, J.H., Glimberg, S.L., *Near-wellbore modeling of a horizontal well with Computational Fluid Dynamics*, Journal of Petroleum Science and Engineering 160/2018, 119–128.

- [23] Tkaczenko A., *Studnie wiercone – część druga*, Wydawnictwo Geologiczne, Warszawa 1971.
- [24] Urbański A., Podleś K., *The 2D/3D method of filtration and stability analysis of a slope with dewatering wells*, ZSoil Days, Lausanne 2017, https://www.zsoil.com/zsoil_day/2017/Urbanski-Podles_Wells_2D_3D.pdf (access: 15.10.2018).
- [25] Urbański A., *Multi-scale analysis of a flow to drainage tubes*. ZSoil Days, Lausanne 2016, http://www.zsoil.com/zsoil_day/2016/A_Urbanski_Multi-scale_analysis.pdf (access: 15.10.2018).
- [26] [Wilk B.K., *Ultrafiltration membranes made of: polyaniline, ionic liquid and cellulose*, Technical Transactions 1-Ś/2016, 171–187.
- [27] Yeh H.D., Chang Y.C., *Recent advances in modeling of well hydraulics*, Advances in Water Resources 51/2013, 27–51.

